mAbs 6:3, 689–696; May/June 2014; © 2014 Landes Bioscience

Quantitative cumulative biodistribution of antibodies in mice

Effect of modulating binding affinity to the neonatal Fc receptor

Victor Yip[1], Enzo Palma[1], Devin B Tesar[2], Eduardo E Mundo[1], Daniela Bumbaca[1], Elizabeth K Torres[3], Noe A Reyes[1], Ben Q Shen[1], Paul J Fielder[1], Saileta Prabhu[1], Leslie A Khawli[1†] and C Andrew Boswell[1,*]

[1]Preclinical and Translational Pharmacokinetics; Genentech Research & Early Development; South San Francisco, CA USA; [2]Drug Delivery Department; Pharma Technical Development, Genentech; South San Francisco, CA USA; [3]Non-Clinical Operations; Genentech Research & Early Development; South San Francisco, CA USA

[†]Current address: University of Southern California; Keck School of Medicine; Department of Pathology; Los Angeles, CA USA

Keywords: FcRn, biodistribution, pharmacokinetics, radiolabeled, metabolism, indium

The neonatal Fc receptor (FcRn) plays an important and well-known role in antibody recycling in endothelial and hematopoietic cells and thus it influences the systemic pharmacokinetics (PK) of immunoglobulin G (IgG). However, considerably less is known about FcRn's role in the metabolism of IgG within individual tissues after intravenous administration. To elucidate the organ distribution and gain insight into the metabolism of humanized IgG1 antibodies with different binding affinities FcRn, comparative biodistribution studies in normal CD-1 mice were conducted. Here, we generated variants of herpes simplex virus glycoprotein D-specific antibody (humanized anti-gD) with increased and decreased FcRn binding affinity by genetic engineering without affecting antigen specificity. These antibodies were expressed in Chinese hamster ovary cell lines, purified and paired radiolabeled with iodine-125 and indium-111. Equal amounts of I-125-labeled and In-111-labeled antibodies were mixed and intravenously administered into mice at 5 mg/kg. This approach allowed us to measure both the real-time IgG uptake (I-125) and cumulative uptake of IgG and catabolites (In-111) in individual tissues up to 1 week post-injection. The PK and distribution of the wild-type IgG and the variant with enhanced binding for FcRn were largely similar to each other, but vastly different for the rapidly cleared low-FcRn-binding variant. Uptake in individual tissues varied across time, FcRn binding affinity, and radiolabeling method. The liver and spleen emerged as the most concentrated sites of IgG catabolism in the absence of FcRn protection. These data provide an increased understanding of FcRn's role in antibody PK and catabolism at the tissue level.

Introduction

Advances in monoclonal antibody (mAb) engineering, including phage-display technologies, have enabled the development of humanized, i.e., mouse complementarity determining region (CDR) residues grafted on to a human framework residues, as well as fully human antibodies with desirable pharmacokinetic (PK) and biodistribution properties.[1] These engineered mAbs have been mass-produced as highly specific reagents used across many clinical settings, including oncology, inflammation, infectious diseases, transplantation and cardiovascular medicine.[2] The unique CDR usually defines an antibody's binding site, i.e., antigen specificity, and resides in the variable fragment (Fv) portion of the molecule.

In immunoglobulin G (IgG), the Fc domain regulates antibody-based therapy by binding to Fc gamma receptors (FcγR) and eliciting immune effector functions.[3] Another characteristic of the Fc portion, specifically the CH2-CH3 domain, has the ability to bind to the neonatal Fc receptor (FcRn) with high affinity at acidic pH, but with very low affinity at neutral, i.e., plasma, pH.[4,5] This scenario enables IgG to be bound by FcRn in the acidic environment of the sorting endosome (pH ≤ 6.0) in endothelial cells and to be recycled back into circulation where dissociation occurs under more alkaline (pH > 7) conditions.[6] The population of IgG that is not bound to FcRn in the endosome undergoes transport to, and proteolysis in, the lysosomes.[5] It has been well-established that the strict pH dependence of this IgG/FcRn interaction is responsible for protecting mAbs from degradation.[7,8] Consequently, FcRn plays an important role in IgG catabolism[5,9] and accounts for the persistence of IgG in the circulation of rodents and higher species.[10,11] Also known as the major histocompatibility complex class I-related receptor,

*Correspondence to: C Andrew Boswell; Email: boswell.andy@gene.com
Submitted: 01/24/2014; Revised: 02/26/2014; Accepted: 02/27/2014; Published Online: 03/05/2014
http://dx.doi.org/10.4161/mabs.28254

Table 1. Affinity measurements of anti-gD variant binding to mFcRn by surface plasmon resonance

Variant	k_{on} ($M^{-1}s^{-1}$)	k_{off} (s^{-1})	K_D (nM)
IgG1 WT	6160	0.0037	601
IgG1 $FcRn^+$	19100	0.0021	108
IgG1 $FcRn^-$	1230	0.1146	93000

FcRn possesses additional roles for protecting serum albumin from degradation[12] and in the passive delivery of IgG from mother to young, i.e., IgG in milk absorbed through gut.[13] Accordingly, FcRn is expressed widely in endothelial, epithelial and hematopoietic cells including organs such as skin, muscle, kidney, liver, and placenta.[5,14-16]

The fact that half-life of an IgG in vivo can be influenced by altering its binding affinity to FcRn at different pH is well-established.[5] Several studies have shown a correlation between the serum half-life and binding affinity of IgGs for FcRn.[10,17-19] However, this correlation is not always observed, as different human IgG subclasses exhibit different in vivo half-lives, but appear to bind human FcRn with K_D values that are within the same order of magnitude.[20,21] A possible explanation of these discrepancies is that the ratio of IgG protected/destroyed depends not only on the affinity of FcRn, but also on the competition between the binding of IgG to FcRn and its intracellular degradation prior to its interaction with FcRn.[9] It has also been reported that several IgG Fc variants that bind stronger to FcRn at pH > 7 have shorter in vivo half-lives compared with the corresponding wild-type (WT) IgG because they cannot dissociate from FcRn.[22,23] An ideal IgG Fc variant should possess increased FcRn affinity at acidic pH compared with a WT antibody, thus retaining binding while in the endosome, and having weaker or equivalent affinity at pH > 7 to facilitate release back into systemic circulation.[10,22,23]

PK and tissue biodistribution studies play an important role in determining specific and non-specific tissue accumulation of radiolabeled IgGs in rodent models. Disposition characteristics are important parameters to consider when designing and testing novel mAbs because they can help predict or explain target-mediated disposition, toxicity, or off-target effects. Although the effects of FcRn binding on systemic PK are well-established, considerably less is known about the catabolic fates of FcRn binding variants within individual tissues. Instead of directly affecting IgG distribution from blood to tissues, i.e., target-mediated clearance, cellular FcRn is expected to influence the intracellular fates of the endocytosed antibodies based on their relative abilities to bind FcRn and thus be rescued from lysosomal degradation. To examine the potential effects of altering FcRn binding affinity on IgG tissue PK and metabolism in more detail, we engineered two humanized anti-glycoprotein D Fc variants (H310Q and T307Q/N434A, EU numbering) with different binding affinities to mFcRn and compared their biodistributions to that of the WT antibody in mice. Furthermore, we chose to evaluate these antibodies radiolabeled with both iodine-125 (non-residualizing) and indium-111 (residualizing) radionuclides to obtain information regarding both distribution and metabolism. The differences in biodistribution patterns of these two labeling methods is driven by their cellular metabolisms, after which I-125-containing catabolites undergo cellular efflux and systemic (primarily urinary) clearance whereas the more polar In-111 catabolites (mostly metal-chelate-amino acid adducts) have an enhanced retention within cells. Given the importance of pH-dependent interactions to the efficient recycling of an IgG, these studies have been designed to gain a better understanding of the relationships among FcRn binding affinity, systemic PK, biodistribution, and cellular metabolism of antibodies in tissues.

Results

mFcRn affinity assessment by surface plasmon resonance

The T307Q/N434A variant (designated henceforth as $FcRn^+$), showed a roughly 5-fold increase in binding affinity to murine FcRn relative to the wild-type anti-gD (IgG1 WT), consistent with previous findings for another antibody bearing the same mutation (**Table 1**).[10]

Radiochemistry

The radiochemical yields of the ^{125}I-labeled antibodies used in the studies were 68% for WT, 66% for $FcRn^+$ and 61% for $FcRn^-$. The specific activities of the ^{125}I-labeled antibodies used in the studies were 10.00 μCi/μg for WT, 10.49 μCi/μg for $FcRn^+$ and 9.43 μCi/μg for $FcRn^-$. The radiochemical yields of the ^{111}In-labeled antibodies used in the studies were 72% for WT, 76% for $FcRn^+$ and 79% for $FcRn^-$. The specific activities of the ^{111}In-labeled antibodies used in the studies were 17.0 μCi/μg for WT, 14.0 μCi/μg for $FcRn^+$ and 20.8 μCi/μg for $FcRn^-$. Size-exclusion HPLCs of all radiolabeled antibodies are included in the Supporting Information.

Plasma pharmacokinetics

After intravenous administration of human IgG1 with various binding affinities to murine FcRn, the plasma concentrations of the WT and $FcRn^+$ variant declined in a biphasic manner, whereas the $FcRn^-$ variant's clearance was more rapid and at least biphasic (possibly triphasic). The plasma concentrations, expressed in percentage of injected dose per milliliter (%ID/mL), at 15 min post-dose were similar across antibodies. Specifically, concentrations of the ^{125}I-labeled antibodies were 78 ± 8, 74 ± 8, and 68 ± 13%ID/mL for IgG1 WT, $FcRn^+$, and $FcRn^-$, respectively (**Fig. 1A**). Similarly, concentrations of the respective ^{111}In-labeled antibodies were 76 ± 6, 70 ± 7, and 68 ± 13%ID/mL (**Fig. 1B**). By 24 h post-dose, plasma concentrations of the $FcRn^-$ variant had decreased more rapidly than IgG1 WT and $FcRn^+$, with a concentration of 8.8 ± 0.5%ID/mL for ^{125}I-labeled $FcRn^-$ compared with 27 ± 2 and 26 ± 3%ID/mL for IgG1 WT and $FcRn^+$, respectively (**Fig. 1A**). A similar trend was observed in the plasma concentrations of ^{111}In-labeled variants and continued to the end of the study (**Fig. 1B**). The differences between IgG1 WT and $FcRn^+$ were insignificant as the plasma concentration at 14 d post-dose showed similar values. For instance, the concentrations of ^{125}I-labeled IgG1 WT and $FcRn^+$ were 6.2 ± 5.2 and 6.6 ±

3.2%ID/mL, respectively (**Fig. 1A**). The respective values for the ^{111}In-labeled variants were 7.3 ± 6.5 and 7.9 ± 2.6%ID/mL (**Fig. 1B**).

The plasma exposures were generally similar between IgG WT and FcRn$^+$, but different for FcRn$^-$. Specifically, the plasma AUC_{0-7} values from ^{125}I data were 164 ± 5, 169 ± 14 and 43 ± 1%ID*day/mL for IgG1 WT, FcRn$^+$, and FcRn$^-$, respectively (**Table 2**). In a similar trend, plasma AUC_{0-7} values derived from ^{111}In data were 182 ± 3, 182 ± 10 and 95 ± 1%ID*day/mL for IgG1 WT, FcRn$^+$, and FcRn$^-$, respectively. The PK of ^{125}I- and ^{111}In-labeled variants corresponded generally well with each other except in the case of the FcRn$^-$ variant, for which the ^{111}In-labeled variant appeared to clear more slowly than the ^{125}I-labeled variant.

Tissue distribution

The radioactivity measured from each tissue was calculated into the percentage of injected dose normalized by the tissue weight in grams (%ID/g). The tissue distribution of the non-residualizing ^{125}I-labeled antibodies at 6 h post-dose revealed distribution to multiple blood rich tissues such as liver, lungs, kidneys and heart (**Fig. 2**). However, there were slight differences between the three variants, especially for the FcRn$^-$ variant that also showed significantly faster blood clearance. The tissue distribution of the ^{111}In-labeled antibodies at 6 h post-dose were similar to that of the ^{125}I-labeled antibodies for all variants (**Fig. 2A and B**). By 24 h post-dose, all of the collected tissues for the ^{125}I-labeled FcRn$^-$ variant contained significantly lower radioactive uptake compared with the IgG1 WT variant (**Fig. 2C**). This same observation for the ^{125}I-labeled FcRn$^-$ variant persisted at 168 h post-dose (**Fig. 2E**). Fewer significant differences were observed between the ^{111}In-labeled WT and FcRn$^-$ variant relative to the ^{125}I-labeled counterparts, especially at 24 h (**Fig. 2D**); this reflects the fact that, unlike ^{125}I, ^{111}In is a residualizing label that accumulates within tissues long after the lysosomal degradation of the original radiolabeled molecule. Because of the residualizing effect of the ^{111}In-DOTA complex, most tissue levels of ^{111}In remained relatively constant between 6 and 24 h (**Fig. 2A-D**). Splenic uptake of the ^{111}In-labeled FcRn$^-$ variant increased from 6.0 ± 1.6%ID/g at 6 h to 9.7 ± 3.5%ID/g at 24 h (**Fig. 2B and D**). Considerably higher uptake of ^{111}In than ^{125}I was observed in many tissues, particularly the liver and spleen, at 168 h post-dose, and this was especially true for the FcRn$^-$ variant (**Fig. 2E and F**). Overall, the trends in tissue distribution between the FcRn$^+$ and IgG1 WT were largely similar irrespective of labeling method (**Fig. 2**). An interesting exception, however, was that the radioactive uptake of both ^{125}I and ^{111}In in brain at 168 h was roughly 2-fold higher for the FcRn$^+$ variant (^{125}I: 0.25 ± 0.24%ID/g and ^{111}In: 0.41 ± 0.05%ID/g) than for the IgG WT (^{125}I: 0.12 ± 0.06%ID/g and ^{111}In: 0.22 ± 0.06) (**Fig. 2E and F**, insets). However, no such difference in brain uptake between the IgG WT and FcRn$^+$ variants was observed at 24 h (**Fig. 2C and D**, insets).

The distribution data was further analyzed to estimate the area under the tissue concentration–time curve from zero to seven days (AUC_{0-7}) for each tissue. The AUC_{0-7} values generated by the ^{125}I data were similar between IgG WT and FcRn$^+$ in all tissues while FcRn$^-$ was significantly lower (**Table 2**). A similar trend

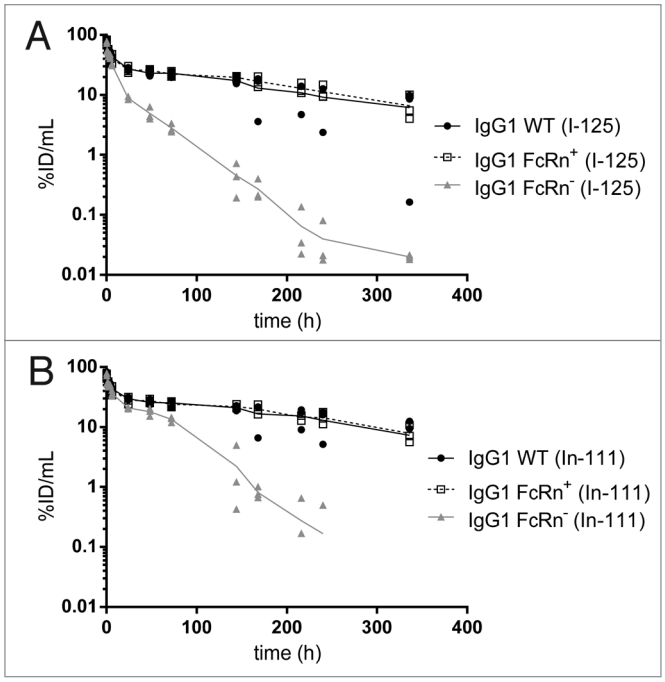

Figure 1. Plasma pharmacokinetic curves of the IgG1 WT, FcRn$^+$, and FcRn$^-$ variants radiolabeled with (**A**) iodine-125 and (**B**) indium-111.

was observed for the ^{111}In data, except that uptake of radioactivity in the liver and spleen was much higher for the FcRn$^-$ compared with the IgG WT and FcRn$^+$ (**Table 2**). This is a critical finding since the liver and spleen are both FcRn-expressing tissues that would afford protection from metabolism to FcRn-binding antibodies. This opposite trend between ^{125}I and ^{111}In uptake data is further highlighted from the ratios of AUC_{0-7} from the liver and spleen compared with that of the plasma; these ratios were 0.64 and 0.56, respectively, whereas ratios of < 0.3 were observed for all other tissues (**Fig. 3**). Furthermore, kidneys, heart, large intestine, small intestine, and skin are also FcRn-expressing organs. They would metabolize the FcRn$^-$ variant much more readily than WT IgG or the FcRn$^+$ variant, and this is indeed confirmed by the larger tissue:plasma (AUC_{0-7}) ratios in terms of the cumulative ^{111}In signal (**Fig. 3B**).

Discussion

Characterization of the tissue PK and metabolism of IgGs is essential for understanding the mechanisms regulating the steady-state concentrations of antibodies in the circulation.[24] Accordingly, our experiments using indium-111-labeled IgGs provide a more direct approach for identifying the sites of cumulative distribution and potential catabolism of IgG under physiological conditions. It is difficult to argue from the ^{125}I-labeled IgG data alone that any one tissue has a dominant role in the metabolism of IgG, since it is simultaneously proposed that ^{125}I-labeled degradation products are being rapidly exocytosed or diffused from this tissue.[25] As such, alternative residualizing

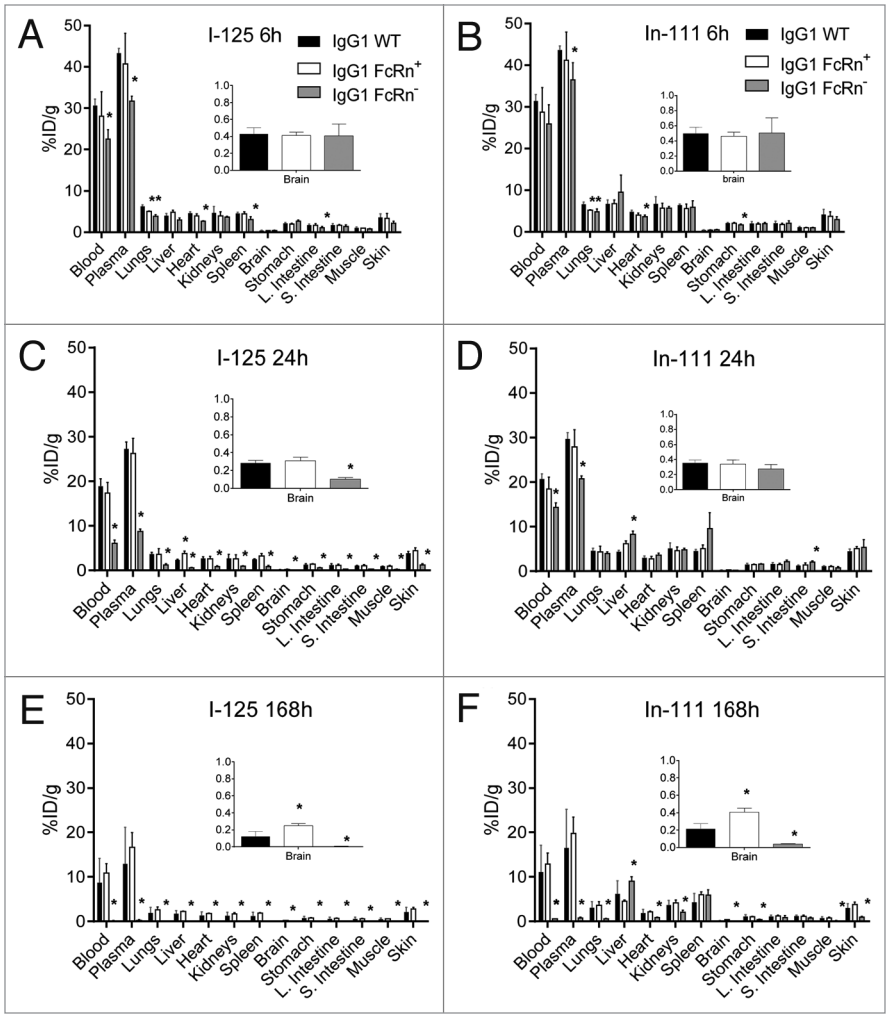

Figure 2. Tissue distribution at 6 (**A and B**), 24 (**C and D**), and 168 (**E and F**) hours of the IgG1 WT, FcRn$^+$, and FcRn$^-$ variants radiolabeled with iodine-125 (**A, C and E**) and indium-111 (**B, D and F**). Asterisks represent significant ($P < 0.05$) differences relative to WT by unpaired *t* test.

labels for studying IgG distribution, which are more efficiently retained in tissues, should permit a more definitive assessment of the role of various tissues in IgG tissue catabolism.[26] Indium-111 labeling via the chelating agent, DOTA, has been widely used in tissue distribution studies of proteins.[27] The ^{111}In-DOTA label is entirely satisfactory as a residualizing radiolabel; therefore PK analyses of tissue distribution of ^{111}In-DOTA-IgG complex have been developed. In this approach, after catabolism, radioactive metabolites that are charged[28] and hydrophilic are unable to pass through biological barriers such as the plasma and lysosomal membranes, promising the retention of radioactivity within the cells that have taken up the radiolabeled compound.

An important aspect of FcRn is that its biological function, at least in terms of IgG interaction, is essentially limited to the intracellular environment due a strict pH dependence. Even though the role of FcRn as a recycling receptor suggests that it does indeed come in contact with the extracellular fluid, it is only to release IgG (pH > 7), whereas binding can only occur in lysosomes or other endocytic compartments (pH ≤ 6) (**Fig. 4**).

Several studies have now demonstrated that maintaining low binding affinity of IgG to FcRn at pH 7.4 is as essential as the increased binding affinity at pH ≤ 6.0 for efficient recycling and serum persistence of IgG.[10,22,23] FcRn protects IgG from intracellular catabolism and has been shown to be capable of transporting IgG across cell monolayers in both the apical-to-basolateral and basolateral-to-apical direction.[5,29] Accordingly, unlike many cell surface receptors recognized by antibody complementarity-determining regions (CDRs), cellular FcRn should not be expected to influence the targeting of IgG to most tissues. As such, one should assume that all three IgG1 variants, WT, FcRn$^+$, and FcRn$^-$, should possess equal abilities to distribute to tissues and enter cells, via blood vessel extravasation and fluid pinocytosis, respectively. Any differential readout in radioactivity should therefore be driven by the intracellular fates of the endocytosed antibodies based on their relative abilities to bind FcRn and their ensuing cellular trafficking.

The plasma PK data for the IgG1 WT, FcRn$^+$, and FcRn$^-$ variants (**Fig. 1**, **Table 2**) were consistent with previously reported data for similar variants.[4,30] The lack of improvement in PK for the FcRn$^+$ IgG variant relative to WT could be due to the species-specific nature of FcRn binding.[31,32] Specifically, human IgG is bound by murine FcRn with higher affinity than by human FcRn. As a result, the enhancement of receptor binding for the FcRn$^+$ variant is more modest for mFcRn than for hFcRn (6-fold and 10-fold, respectively).[10] In addition, the possibility exists that the FcRn$^+$ variant exhibits increased binding to mFcRn at both acidic and basic pH, resulting in incomplete dissociation of mFcRn-IgG complexes at the cell surface following recycling.

The ^{111}In-labeled FcRn$^-$ variant appeared to clear more slowly from plasma than the corresponding ^{125}I-labeled variant. We speculate that this phenomenon is due to transchelation of In(III), having similar coordination properties as Fe(III), from DOTA into transferrin (or other iron-containing plasma proteins) during the period of rapid distribution to tissues and subsequent pinocytosis. Although the thermodynamic stability of In(III)-DOTA is higher than In(III)-transferrin,[33] cellular metabolism of the extremely rapidly clearing FcRn$^-$ variant may produce sufficiently high local concentrations of ^{111}In-containing catabolites to kinetically favor partial transchelation from DOTA to transferrin, especially within acidic lysosomes. However, for the vast majority of antibodies having typical PK, we have observed very similar blood clearance data for ^{111}In- and ^{125}I-derived molecules.[27,34,35]

Table 2. Tissue AUC_{0-7} (day*%ID/mL) for anti-gD variants

Variant	Label	Plasma	Lungs	Liver	Kidney	Heart	Spleen	Stomach	Large Intestine	Small Intestine	Brain	Muscle	Skin
IgG1 WT	^{125}I	164 ± 5.38	21.5 ± 1.20	15.5 ± 0.575	15.4 ± 2.14	15.5 ± 0.692	14.6 ± 0.340	8.01 ± 0.425	7.09 ± 0.591	6.36 ± 0.268	1.55 ± 0.0900	5.43 ± 0.0946	21.5 ± 1.53
	^{111}In	182 ± 2.76	28.3 ± 1.34	37.2 ± 1.60	32.1 ± 2.45	18.5 ± 0.758	31.6 ± 2.00	9.79 ± 0.575	10.1 ± 0.649	9.16 ± 0.502	2.09 ± 0.0923	6.85 ± 0.243	26.6 ± 1.15
IgG1 FcRn$^+$	^{125}I	169 ± 14.0	22.8 ± 3.30	22.1 ± 1.30*	16.1 ± 2.10	16.3 ± 1.25	18.8 ± 1.32*	8.18 ± 0.401	6.92 ± 0.636	6.55 ± 0.626	2.00 ± 0.122*	5.72 ± 0.353	25.2 ± 1.82
	^{111}In	182 ± 9.97	28.3 ± 2.85	37.8 ± 1.48	31.2 ± 2.02	18.3 ± 1.09	38.1 ± 1.95*	9.63 ± 0.323	10.0 ± 0.628	9.35 ± 0.971	2.59 ± 0.139*	6.67 ± 0.449*	30.7 ± 1.26*
IgG1 FcRn$^-$	^{125}I	43.1 ± 1.16*	6.63 ± 0.500*	3.77 ± 0.220*	5.46 ± 0.131*	4.46 ± 0.407*	4.60 ± 0.544*	3.63 ± 0.100*	1.76 ± 0.132*	2.00 ± 0.104*	0.58 ± 0.0485*	1.52 ± 0.124*	5.89 ± 0.490*
	^{111}In	94.5 ± 1.46*	17.8 ± 0.821*	60.0 ± 2.41*	25.6 ± 1.02*	16.8 ± 0.923	53.3 ± 7.16*	7.58 ± 0.278*	11.1 ± 1.00	10.7 ± 0.598*	1.30 ± 0.121*	4.01 ± 0.423*	22.6 ± 3.41

Significant ($P < 0.05$) differences by unpaired t test are indicated by asterisks and are relative to IgG WT for the corresponding radionuclide.

As for the tissue distribution data, our major finding that liver and spleen are the major sites of IgG catabolism in rodents is consistent with earlier work.[24] It should be noted, however, that although liver and spleen are important on a tissue mass-normalized basis, the skin and muscle are actually more important since they comprise a greater percentage of body weight.[36] Relatively few studies have been reported on the effect of FcRn on tissue distribution. Ferl and colleagues described the use of ^{111}In- and ^{125}I-labeled single-chain Fv-Fc antibody fragments, concluding that liver, skin, and muscle play pivotal roles in IgG catabolism.[37] Jaggi and coworkers explored the tissue distribution in a limited number of tissues (liver, kidney, spleen) of an IgG in both wild-type and FcRn$^{-/-}$ mice, reporting a trend consistent with our findings of decreased renal uptake and increased hepatic uptake of radioactivity in the absence of FcRn protection at a comparable time point (160 h).[38] Garg and Balthasar reported the tissue concentrations of an IgG in wild-type and FcRn$^{-/-}$ mice, but the study was limited to a non-residualizing ^{125}I labeling method.[39]

Abuqayyas and Balthasar recently reported a lack of evidence for a role of FcRn in antibody distribution to the brain using an ^{125}I-labeled antibody in wild-type vs. FcRn$^{-/-}$ mice.[40] This is consistent with an earlier report from the same group.[41] Although our current data showed higher brain uptake at 168 h for the FcRn$^+$ variant relative to WT in terms of both ^{125}I and ^{111}In (see **Fig. 2E and F**, insets), this trend was absent at other time points and did not translate into higher overall brain exposures (**Fig. 3**, insets). Others have postulated that higher brain concentrations of variants with enhanced binding to FcRn could result from a role in efflux of IgG, as opposed to influx.[42,43] Further evidence toward this notion is the fact that brain expression of FcRn is co-localized with the Glut1 glucose transporter in the capillary endothelium, suggesting that FcRn is expressed in the proper location to potentially mediate reverse transcytosis of IgG from brain to blood.[44]

A physiologically-based PK (PBPK) model incorporating the protective role of FcRn predicted that the skin is one of the major organs responsible for IgG catabolism in mice, accounting for approximately 33% of the total IgG elimination.[39] This finding is also supported by evidence of FcRn expression on the endothelium of the large vascular beds of skin in mice.[15] Indeed, our data for both the wild-type IgG and enhanced FcRn binding variant demonstrate that the skin has roughly triple the uptake of muscle (**Fig. 2**), despite the two tissues having a similar vascular volume. In the absence of FcRn protection, however, the liver and spleen emerge as the major sites of antibody catabolism.

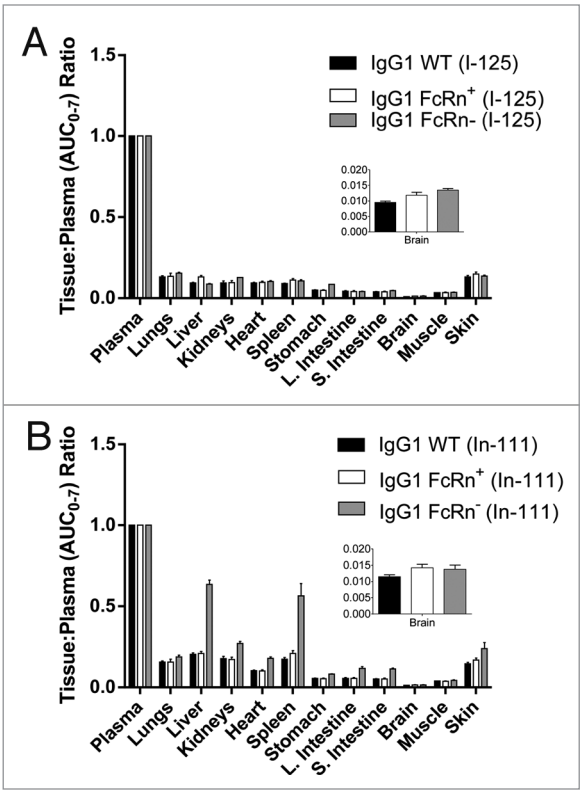

Figure 3. Ratios of tissue AUC_{0-7} to plasma AUC_{0-7} of the IgG1 WT, FcRn$^+$, and FcRn$^-$ variants radiolabeled with (**A**) iodine-125 and (**B**) indium-111. The abbreviation AUC_{0-7} denotes the area under the concentration-time curve from 0 to 7 d. Note that AUC values for indium-111-labeled antibodies do not reflect true exposure of intact antibody since indium-111 is a residualizing radiometal label (**Fig. 4**).

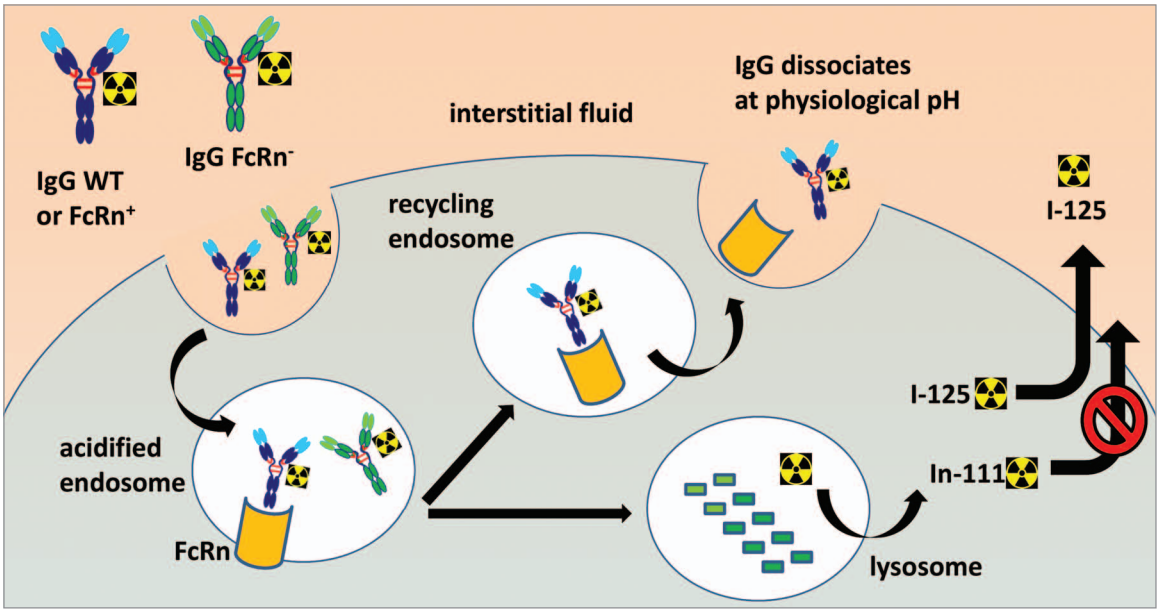

Figure 4. Schematic diagram of the cellular processing of radiolabeled IgG in the presence and absence of FcRn binding affinity. Both ^{125}I- and ^{111}In-DOTA-labeled antibodies enter the cell by pinocytosis. In the sorting endosome, FcRn-protected IgG is recycled back to the extracellular space, while non-protected IgG proceeds to lysosomal proteolytic degradation. The radiolabeled catabolite, ^{111}In-DOTA-lysine, is residualizing due to its polarity or charge and tends to accumulate within cells. In contrast, radioiodinated protein catabolites are rapidly effluxed from cells.

In conclusion, we augmented the FcRn binding affinity of herpes simplex virus glycoprotein D-specific antibody (humanized anti-gD) by genetic engineering to measure both the real-time IgG uptake (I-125) and cumulative uptake of IgG and catabolites (In-111) in individual tissues up to 7 d post injection. The PK and distribution of the wild-type IgG and the variant with enhanced binding for FcRn were largely similar to each other, but vastly different for the low-FcRn-binding variant due to its very low systemic exposure. Uptake in individual tissues varied across time, FcRn binding affinity, and radiolabeling method. The liver and spleen emerged as the most concentrated sites of IgG catabolism in the absence of FcRn protection. These data provide an increased understanding of FcRn's role in antibody tissue PK and catabolism.

Materials and Methods

mFcRn affinity assessment by surface plasmon resonance

The binding affinity of the high affinity Soluble murine FcRn (mFcRn) was expressed and purified from Chinese hamster ovary cells as reported previously.[10] The binding affinity of mFcRn for WT IgG1 and the high- and low-affinity FcRn binding variants was measured at pH 5.8 by surface plasmon resonance using a Biacore T-200TM instrument (GE Healthcare). The variants were immobilized onto a CM5 Series S sensor chip and 12 serial dilutions of mFcRn were injected for 60 s at a flow rate of 50 μL/min. Following each mFcRn injection the surface was regenerated by two 30 s injections of pH 8.0 buffer to dissociate bound mFcRn. Raw sensogram data were reduced and referenced using the Scrubber II software package (BioLogic Software) and fit to a simple 1:1 binding model.

Antibody variants

The humanized IgG1 anti-herpes simplex virus glycoprotein D antibody (wild-type anti-gD, designated henceforth as IgG1 WT) was obtained from Genentech, Inc. as previously described.[34] Two antibody variants were produced from the wild-type IgG1 based on knowledge that Fc residues Thr307, Asn434 and His310 are all critical for IgG interaction with FcRn in mice.[8,45-47] A variant with enhanced binding affinity for FcRn, T307Q/N434A (designated henceforth as FcRn$^+$), was selected based on previous demonstration of a 5-fold increase in binding affinity to murine FcRn.[10] A null binding variant, H310Q (designated henceforth as FcRn$^-$), was also selected since His310 is highly conserved and important for the pH-dependent binding to FcRn across different species.[10]

Radiochemistry

Antibodies were conjugated to 1,4,7,10-tetraazacyclododecane-*N*,*N*',*N*,"*N*""-tetraacetic acid (DOTA) for indium-111 (^{111}In) complexation by random modification of lysine residues as previously described.[34,35,48] Antibodies were radioiodinated using an indirect iodogen addition method.[49] The radiolabeled proteins were purified using NAP5™ columns (GE Healthcare Life Sciences, cat. 17–0853–01) pre-equilibrated in PBS. All radiolabeled antibodies were characterized by size-exclusion high-performance liquid chromatography with in-line radiometric and UV detectors to compare the profiles of radioimmunoconjugates and corresponding unlabeled antibodies.

Tissue distribution and pharmacokinetics

All animals were handled in accordance with IACUC guidelines. Female CD1 mice ranging from 6 to 8 wk old and

weighing approximately 20 g at the initiation of the study were randomized into groups. At 1 and 24 h prior to dosing, all mice received a 100 μL intraperitoneal injection of 30 mg/mL sodium iodide to prevent iodine-125 (^{125}I) sequestration in the thyroid. Equal amounts of radioactivity for ^{125}I-labeled and ^{111}In-DOTA-labeled antibodies (5 μCi each) were mixed with the corresponding unlabeled antibody at 5 mg/kg and administered intravenously by bolus tail vein injection. Whole blood was collected via retro-orbital bleed under isoflurane anesthesia at pre-selected time points up to 14 d (n = 3) from staggered mice. Blood samples were processed for plasma and stored at -70 °C until analysis. The following tissues were harvested terminally at 6 h, 1 d and 7 d: liver, lungs, kidneys, heart, spleen, stomach, small intestine, large intestine, brain, skin, and muscle. Tissues were also collected at 14 d, but these data are not reported because accurate counting of ^{111}In (2.8 d decay half-life) was difficult in some groups/tissues at this late time point. All tissues were rinsed with phosphate buffered saline, blot-dried, weighed, frozen on dry ice, and stored at -70 °C until radiometric analysis. It should be noted that neither perfusion nor mathematical correction of residual blood from tissues was performed.

Radioactivity counts were obtained from plasma and tissue samples using a Wallac 1480 Wizard 3 automatic gamma counter (EC&G Wallac, cat. 1480–011). Radioactive counts were converted to dose-normalized concentrations by calculating the percentage of injected dose per gram of tissue (or milliliter of blood or plasma). Plasma concentration–time data was used to estimate the area under the curve from zero to seven days ($AUC_{0–7}$) by using a non-compartmental analysis method (NCA) using sparse sampling with WinNonlin software (v 5.2.1 Pharsight Corporation). Calculation of $AUC_{0–7}$ in lieu of $AUC_{0–14}$ was performed for two reasons: (1) low counts of ^{111}In (2.8-d decay half-life), with selected groups approaching the detection limit of the gamma counting assay; and (2) likely (but unconfirmed) anti-therapeutic antibody (ATA) formation leading to fast clearance (signified by low levels of radioactivity in plasma and tissues) in selected animals. Tissue concentration–time data was also analyzed by using NCA with sparse sampling with WinNonlin software to estimate the area under the curve from zero to seven days ($AUC_{0–7}$). Standard errors in $AUC_{0–7}$ were calculated by the method of Bailer.[50]

Disclosure of Potential Conflicts of Interest

All authors are employees of Genentech, a member of the Roche Group, and hold financial interest in Hoffmann-La Roche. All financial support was provided by Genentech.

Acknowledgments

We thank Andy Yeung, Henry Lowman, Rong Deng, Jaime Anguiano and Simon Williams for helpful discussions. We also acknowledge Sheila Ulufatu, Jason Ho, Shannon Stainton, Bernadette Johnstone, Cynthia Young, Kirsten Messick, Jose Imperio, Maria Duran, Mayra Monett, Nina Ljumanovic, Roxanne Vega, Nicole Valle, and Michelle Schweiger for animal studies support.

Supplemental Materials

Supplemental materials may be found here:
www.landesbioscience.com/journals/mabs/article/28254

References

1. Sidhu SS. Full-length antibodies on display. Nat Biotechnol 2007; 25:537-8; PMID:17483836; http://dx.doi.org/10.1038/nbt0507-537
2. Brekke OH, Sandlie I. Therapeutic antibodies for human diseases at the dawn of the twenty-first century. Nat Rev Drug Discov 2003; 2:52-62; PMID:12509759; http://dx.doi.org/10.1038/nrd984
3. Lobo ED, Hansen RJ, Balthasar JP. Antibody pharmacokinetics and pharmacodynamics. J Pharm Sci 2004; 93:2645-68; PMID:15389672; http://dx.doi.org/10.1002/jps.20178
4. Kim JK, Tsen MF, Ghetie V, Ward ES. Catabolism of the murine IgG1 molecule: evidence that both CH2-CH3 domain interfaces are required for persistence of IgG1 in the circulation of mice. Scand J Immunol 1994; 40:457-65; PMID:7939418; http://dx.doi.org/10.1111/j.1365-3083.1994.tb03488.x
5. Roopenian DC, Akilesh S. FcRn: the neonatal Fc receptor comes of age. Nat Rev Immunol 2007; 7:715-25; PMID:17703228; http://dx.doi.org/10.1038/nri2155
6. Ober RJ, Martinez C, Vaccaro C, Zhou J, Ward ES. Visualizing the site and dynamics of IgG salvage by the MHC class I-related receptor, FcRn. J Immunol 2004; 172:2021-9; PMID:14764666
7. Junghans RP. Finally! The Brambell receptor (FcRB). Mediator of transmission of immunity and protection from catabolism for IgG. Immunol Res 1997; 16:29-57; PMID:9048207; http://dx.doi.org/10.1007/BF02786322
8. Raghavan M, Bonagura VR, Morrison SL, Bjorkman PJ. Analysis of the pH dependence of the neonatal Fc receptor/immunoglobulin G interaction using antibody and receptor variants. Biochemistry 1995; 34:14649-57; PMID:7578107; http://dx.doi.org/10.1021/bi00045a005
9. Ghetie V, Ward ES. Transcytosis and catabolism of antibody. Immunol Res 2002; 25:97-113; PMID:11999172; http://dx.doi.org/10.1385/IR:25:2:097
10. Yeung YA, Leabman MK, Marvin JS, Qiu J, Adams CW, Lien S, Starovasnik MA, Lowman HB. Engineering human IgG1 affinity to human neonatal Fc receptor: impact of affinity improvement on pharmacokinetics in primates. J Immunol 2009; 182:7663-71; PMID:19494290; http://dx.doi.org/10.4049/jimmunol.0804182
11. Roopenian DC, Christianson GJ, Sproule TJ, Brown AC, Akilesh S, Jung N, Petkova S, Avanessian L, Choi EY, Shaffer DJ, et al. The MHC class I-like IgG receptor controls perinatal IgG transport, IgG homeostasis, and fate of IgG-Fc-coupled drugs. J Immunol 2003; 170:3528-33; PMID:12646614
12. Anderson CL, Chaudhury C, Kim J, Bronson CL, Wani MA, Mohanty S. Perspective-- FcRn transports albumin: relevance to immunology and medicine. Trends Immunol 2006; 27:343-8; PMID:16731041; http://dx.doi.org/10.1016/j.it.2006.05.004
13. Ghetie V, Ward ES. Multiple roles for the major histocompatibility complex class I- related receptor FcRn. Annu Rev Immunol 2000; 18:739-66; PMID:10837074; http://dx.doi.org/10.1146/annurev.immunol.18.1.739
14. Montoyo HP, Vaccaro C, Hafner M, Ober RJ, Mueller W, Ward ES. Conditional deletion of the MHC class I-related receptor FcRn reveals the sites of IgG homeostasis in mice. Proc Natl Acad Sci U S A 2009; 106:2788-93; http://dx.doi.org/10.1073/pnas.0810796106; PMID:19188594
15. Borvak J, Richardson J, Medesan C, Antohe F, Radu C, Simionescu M, Ghetie V, Ward ES. Functional expression of the MHC class I-related receptor, FcRn, in endothelial cells of mice. Int Immunol 1998; 10:1289-98; PMID:9786428; http://dx.doi.org/10.1093/intimm/10.9.1289
16. Telleman P, Junghans RP. The role of the Brambell receptor (FcRB) in liver: protection of endocytosed immunoglobulin G (IgG) from catabolism in hepatocytes rather than transport of IgG to bile. Immunology 2000; 100:245-51; PMID:10886402; http://dx.doi.org/10.1046/j.1365-2567.2000.00034.x
17. Datta-Mannan A, Witcher DR, Tang Y, Watkins J, Jiang W, Wroblewski VJ. Humanized IgG1 variants with differential binding properties to the neonatal Fc receptor: relationship to pharmacokinetics in mice and primates. Drug Metab Dispos 2007; 35:86-94; PMID:17050651; http://dx.doi.org/10.1124/dmd.106.011734
18. Ghetie V, Popov S, Borvak J, Radu C, Matesoi D, Medesan C, Ober RJ, Ward ES. Increasing the serum persistence of an IgG fragment by random mutagenesis. Nat Biotechnol 1997; 15:637-40; PMID:9219265; http://dx.doi.org/10.1038/nbt0797-637

19. Suzuki T, Ishii-Watabe A, Tada M, Kobayashi T, Kanayasu-Toyoda T, Kawanishi T, Yamaguchi T. Importance of neonatal FcR in regulating the serum half-life of therapeutic proteins containing the Fc domain of human IgG1: a comparative study of the affinity of monoclonal antibodies and Fc-fusion proteins to human neonatal FcR. J Immunol 2010; 184:1968-76; PMID:20083659; http://dx.doi.org/10.4049/jimmunol.0903296
20. Gurbaxani B, Dela Cruz LL, Chintalacharuvu K, Morrison SL. Analysis of a family of antibodies with different half-lives in mice fails to find a correlation between affinity for FcRn and serum half-life. Mol Immunol 2006; 43:1462-73; PMID:16139891; http://dx.doi.org/10.1016/j.molimm.2005.07.032
21. West AP Jr., Bjorkman PJ. Crystal structure and immunoglobulin G binding properties of the human major histocompatibility complex-related Fc receptor(,). Biochemistry 2000; 39:9698-708; PMID:10933786; http://dx.doi.org/10.1021/bi000749m
22. Dall'Acqua WF, Woods RM, Ward ES, Palaszynski SR, Patel NK, Brewah YA, Wu H, Kiener PA, Langermann S. Increasing the affinity of a human IgG1 for the neonatal Fc receptor: biological consequences. J Immunol 2002; 169:5171-80; PMID:12391234
23. Gan Z, Ram S, Vaccaro C, Ober RJ, Ward ES. Analyses of the recycling receptor, FcRn, in live cells reveal novel pathways for lysosomal delivery. Traffic 2009; 10:600-14; http://dx.doi.org/10.1111/j.1600-0854.2009.00887.x; PMID:19192244
24. Henderson LA, Baynes JW, Thorpe SR. Identification of the sites of IgG catabolism in the rat. Arch Biochem Biophys 1982; 215:1-11; PMID:7092219; http://dx.doi.org/10.1016/0003-9861(82)90272-7
25. Weisbecker U, Ibbotson GE, Livesey G, Williams KE. The fate of homologous 125I-labelled immunoglobulin G within rat visceral yolk sacs incubated in vitro. Biochem J 1983; 214:815-22; PMID:6626158
26. Thorpe SR, Baynes JW, Chroneos ZC. The design and application of residualizing labels for studies of protein catabolism. FASEB J 1993; 7:399-405; PMID:8462781
27. Boswell CA, Bumbaca D, Fielder PJ, Khawli LA. Compartmental tissue distribution of antibody therapeutics: experimental approaches and interpretations. AAPS J 2012; 14:612-8; http://dx.doi.org/10.1208/s12248-012-9374-1; PMID:22648903
28. Boswell CA, Tesar DB, Mukhyala K, Theil FP, Fielder PJ, Khawli LA. Effects of charge on antibody tissue distribution and pharmacokinetics. Bioconjug Chem 2010; 21:2153-63; PMID:21053952; http://dx.doi.org/10.1021/bc100261d
29. Antohe F, Radulescu L, Gafencu A, Ghetie V, Simionescu M. Expression of functionally active FcRn and the differentiated bidirectional transport of IgG in human placental endothelial cells. Hum Immunol 2001; 62:93-105; PMID:11182218; http://dx.doi.org/10.1016/S0198-8859(00)00244-5
30. Deng R, Loyet KM, Lien S, Iyer S, DeForge LE, Theil FP, Lowman HB, Fielder PJ, Prabhu S. Pharmacokinetics of humanized monoclonal anti-tumor necrosis factor-alpha antibody and its neonatal Fc receptor variants in mice and cynomolgus monkeys. Drug Metab Dispos 2010; 38:600-5; http://dx.doi.org/10.1124/dmd.109.031310; PMID:20071453
31. Vaccaro C, Bawdon R, Wanjie S, Ober RJ, Ward ES. Divergent activities of an engineered antibody in murine and human systems have implications for therapeutic antibodies. Proc Natl Acad Sci U S A 2006; 103:18709-14; PMID:17116867; http://dx.doi.org/10.1073/pnas.0606304103
32. Ober RJ, Radu CG, Ghetie V, Ward ES. Differences in promiscuity for antibody-FcRn interactions across species: implications for therapeutic antibodies. Int Immunol 2001; 13:1551-9; PMID:11717196; http://dx.doi.org/10.1093/intimm/13.12.1551
33. Wadas TJ, Wong EH, Weisman GR, Anderson CJ. Coordinating radiometals of copper, gallium, indium, yttrium, and zirconium for PET and SPECT imaging of disease. Chem Rev 2010; 110:2858-902; http://dx.doi.org/10.1021/cr900325h; PMID:20415480
34. Pastuskovas CV, Mundo EE, Williams SP, Nayak TK, Ho J, Ulufatu S, Clark S, Ross S, Cheng E, Parsons-Reponte K, et al. Effects of anti-VEGF on pharmacokinetics, biodistribution, and tumor penetration of trastuzumab in a preclinical breast cancer model. Mol Cancer Ther 2012; 11:752-62; http://dx.doi.org/10.1158/1535-7163.MCT-11-0742-T; PMID:22222630
35. Boswell CA, Mundo EE, Firestein R, Zhang C, Mao W, Gill H, Young C, Ljumanovic N, Stainton S, Ulufatu S, et al. An integrated approach to identify normal tissue expression of targets for antibody-drug conjugates: case study of TENB2. Br J Pharmacol 2013; 168:445-57; http://dx.doi.org/10.1111/j.1476-5381.2012.02138.x; PMID:22889168
36. Wright A, Sato Y, Okada T, Chang K, Endo T, Morrison S. In vivo trafficking and catabolism of IgG1 antibodies with Fc associated carbohydrates of differing structure. Glycobiology 2000; 10:1347-55; PMID:11159927; http://dx.doi.org/10.1093/glycob/10.12.1347
37. Ferl GZ, Kenanova V, Wu AM, DiStefano JJ 3rd. A two-tiered physiologically based model for dually labeled single-chain Fv-Fc antibody fragments. Mol Cancer Ther 2006; 5:1550-8; PMID:16818514; http://dx.doi.org/10.1158/1535-7163.MCT-06-0072
38. Jaggi JS, Carrasquillo JA, Seshan SV, Zanzonico P, Henke E, Nagel A, Schwartz J, Beattie B, Kappel BJ, Chattopadhyay D, et al. Improved tumor imaging and therapy via i.v. IgG-mediated time-sequential modulation of neonatal Fc receptor. J Clin Invest 2007; 117:2422-30; PMID:17717602; http://dx.doi.org/10.1172/JCI32226
39. Garg A, Balthasar JP. Physiologically-based pharmacokinetic (PBPK) model to predict IgG tissue kinetics in wild-type and FcRn-knockout mice. J Pharmacokinet Pharmacodyn 2007; 34:687-709; PMID:17636457; http://dx.doi.org/10.1007/s10928-007-9065-1
40. Abuqayyas L, Balthasar JP. Investigation of the role of FcγR and FcRn in mAb distribution to the brain. Mol Pharm 2013; 10:1505-13; http://dx.doi.org/10.1021/mp300214k; PMID:22838637
41. Garg A, Balthasar JP. Investigation of the influence of FcRn on the distribution of IgG to the brain. AAPS J 2009; 11:553-7; http://dx.doi.org/10.1208/s12248-009-9129-9; PMID:19636712
42. Zhang Y, Pardridge WM. Mediated efflux of IgG molecules from brain to blood across the blood-brain barrier. J Neuroimmunol 2001; 114:168-72; PMID:11240028; http://dx.doi.org/10.1016/S0165-5728(01)00242-9
43. Deane R, Sagare A, Hamm K, Parisi M, LaRue B, Guo H, Wu Z, Holtzman DM, Zlokovic BV. IgG-assisted age-dependent clearance of Alzheimer's amyloid beta peptide by the blood-brain barrier neonatal Fc receptor. J Neurosci 2005; 25:11495-503; PMID:16354907; http://dx.doi.org/10.1523/JNEUROSCI.3697-05.2005
44. Schlachetzki F, Zhu C, Pardridge WM. Expression of the neonatal Fc receptor (FcRn) at the blood-brain barrier. J Neurochem 2002; 81:203-6; PMID:12067234; http://dx.doi.org/10.1046/j.1471-4159.2002.00840.x
45. Kim JK, Firan M, Radu CG, Kim CH, Ghetie V, Ward ES. Mapping the site on human IgG for binding of the MHC class I-related receptor, FcRn. Eur J Immunol 1999; 29:2819-25; PMID:10508256; http://dx.doi.org/10.1002/(SICI)1521-4141(199909)29:09<2819::AID-IMMU2819>3.0.CO;2-6
46. Vaughn DE, Bjorkman PJ. Structural basis of pH-dependent antibody binding by the neonatal Fc receptor. Structure 1998; 6:63-73; PMID:9493268; http://dx.doi.org/10.1016/S0969-2126(98)00008-2
47. Medesan C, Matesoi D, Radu C, Ghetie V, Ward ES. Delineation of the amino acid residues involved in transcytosis and catabolism of mouse IgG1. J Immunol 1997; 158:2211-7; PMID:9036967
48. Boswell CA, Mundo EE, Zhang C, Bumbaca D, Valle NR, Kozak KR, Fourie A, Chuh J, Koppada N, Saad O, et al. Impact of drug conjugation on pharmacokinetics and tissue distribution of anti-STEAP1 antibody-drug conjugates in rats. Bioconjug Chem 2011; 22:1994-2004; http://dx.doi.org/10.1021/bc200212a; PMID:21913715
49. Chizzonite R, Truitt T, Podlaski FJ, Wolitzky AG, Quinn PM, Nunes P, Stern AS, Gately MK. IL-12: monoclonal antibodies specific for the 40-kDa subunit block receptor binding and biologic activity on activated human lymphoblasts. J Immunol 1991; 147:1548-56; PMID:1715362
50. Bailer AJ. Testing for the equality of area under the curves when using destructive measurement techniques. J Pharmacokinet Biopharm 1988; 16:303-9; PMID:3221328; http://dx.doi.org/10.1007/BF01062139